Stochastic μ-Analysis for launcher thrust vector control systems

Andres Marcos, Samir Bennani, Christophe Roux

Abstract Deterministic μ is nowadays very well established in the control analysis community due to its proven capability to perform robust stability and performance analysis for uncertain systems. Nevertheless a common criticism for its use in clearance and certification processes is the lack of quantitative measures on the likelihood occurrence for the identified worst-cases. In addressing this shortcoming, probabilistic μ appeared in the early 1990s but due to the complexity of its calculation it is only recently that toolboxes have started to appear and be used. Probabilistic μ provides a measure of rare events to the worst-case, i.e. they provide upper and lower bounds on the cumulative distribution function of the worst-case gain. In this paper a comparison between deterministic μ and probabilistic μ is presented through their application to the analysis of a study case extracted from the VEGA launcher during the atmospheric phase.

1 Introduction

The Monte Carlo (MC) method is the de facto industrial standard for verification and validation (V&V) processes. It is a very simple indirect simulation-based approach where no analytical representation of the system is really needed or used since the approach performs statistical modeling (i.e. find mean and variance of output) based on random sampling of the inputs to the system. In essence, it empirically estimates the probability distribution that a given requirement satisfies a specific threshold given probability distributions on the parameters. The literature on Monte Carlo is

A. Marcos
University of Bristol, BS8 1TR, United Kingdom e-mail: andres.marcos@bristol.ac.uk

S. Bennani
ESA-ESTEC, Noordwijk, 2201AZ, The Netherlands e-mail: samir.bennani@esa.int

C. Roux
ELV, Rome, 00034, Italy e-mail: Christophe.Roux@elv.it

very extensive since various sampling techniques have been developed depending on the specific area of application.

One of the greatest advantages of MC, besides not requiring specific analytical models, is that the accuracy of the estimates does not depend on the dimension of the parameter space but rather on the number of simulations, which depends on the specified requirements for probability, confidence level and accuracy –i.e. by application of Chernoff/Hoeffding bounds and the Sampling Theorem [22, 5].

On the other hand, its shortcomings are related to: the intensive computational effort, being questionable for maximum/minimum values analysis, and that it is a "soft" bound. The latter means that instead of stating that a requirement is satisfied with a specific probability, i.e. a hard-bound, MC qualifies that that probability is achieved within a specified accuracy and a specified confidence probability [23, 10]. In other words, if you run several MC campaigns each will provide a slightly different answer, thus it is not only important to run a sufficient number of simulations per campaign but also to perform a sufficient number of MC campaigns. Finally, for rare-events (such as worst-cases) the Monte Carlo method will require prohibitively large number of simulations. Thus, as visually presented in reference [12] and more recently in [3], Monte Carlo methods are appropriate for approximating the left part of the curve in Fig. 1.

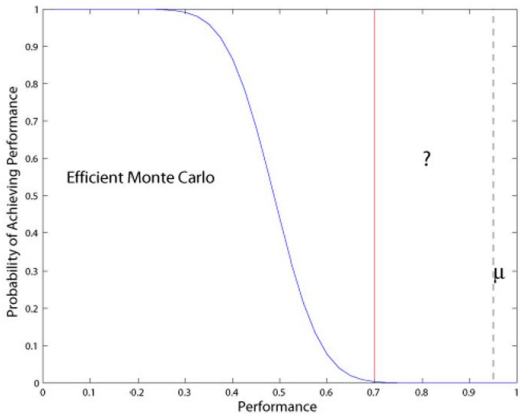

Fig. 1: Monte-Carlo vs Worst-Case methods

In addressing the aforementioned shortcomings, the robust control community has been developing for the last 30 years approaches that provide different and complementary answers to those from Monte Carlo. Knowing that in general the exact computation of the robust stability and performance of a system is intractable due to the exponential growth with the number of parameters, the focus shifted to computing hard-bounds on the objectives. Although for some cases the gap between these bounds might be large it is now accepted after many practical studies, see for

example [11, 4, 18, 9, 17] for aerospace applications, that for most systems the gap is acceptably close to provide a robust assessment after refining the bounds using branch and bounds algorithms [23, 12].

The initial pursuit focused on the (deterministic) structured singular value, μ [6, 1], which is useful in providing an answer to the right most side of Fig. 1. Robustness analysis in the μ-framework is a worst-case paradigm which provides for the entire uncertainty parameter space hard upper and lower bounds on the assessment of the robust stability or performance of a system. The upper bound provides a guaranteed level for the satisfaction of the stability/performance objectives while the lower bound provides a guaranteed level on their violation. Besides the approach providing hard bounds, another of its main strengths is that robust performance problems can be represented as robust stability problems making of μ-analysis a powerful robust analysis framework. Further, the answers provided by μ-analysis provide a level of understanding on the levels of uncertainty and system sensitivity that result in direct information from where to improve the controller as well as from where to better tackle the robustness versus performance trade-off (something lacking in Monte Carlo analysis). On the other hand, the disadvantages are the need to developed specific analytical uncertainty models called Linear Fractional Transformations (LFT) [8] and that it might yield conservative answers in some cases, i.e. the probability of occurrence of the identified worst-case might be exceedingly rare resulting in the risk of rejecting a perfectly valid design based on an almost impossible likelihood of a worst-case.

In addressing the later shortcoming, and the need to be closer to Monte Carlo for industrial and historical legacy purposes, researchers as early as 1990s started to investigate probabilistic-robustness [21, 19] and probabilistic-μ [23, 12, 24]. In both cases, the desire was to provide a quantifiable answer on the probability associated with the robust stability/performance degradation. This is a complementary bridge between Monte Carlo and deterministic μ, since the former empirically estimates the probability of achieving an objective (based on confidence and accuracy levels and sampling of the uncertainty set) while the latter involves computing hard bounds on the satisfaction and violation of the objective over the entire set of uncertainty. With respect to Fig. 1, probabilistic-μ tries to provide an answer for the vertical solid line, i.e. an answer on the distance in performance between the worst-case and the Monte Carlo distribution. Probabilistic-μ assumes that there is some distribution on the uncertainty set (as Monte Carlo) and computes hard bounds (as deterministic-μ) on the resulting probability measure of the objective. The current status on the use of probabilistic-μ is similar to what happened with deterministic-μ, which was developed in the early 1980s [7, 20] but only took off once a consolidated software toolbox was developed [1] almost 20 years later. As mentioned before, research on probabilistic-μ was very active at the end of the 1990s but the lack of a consolidated toolbox, or indeed of a efficient (in terms of computational processing time) and reliable (in terms of quality of the answer) algorithm, damped its development. Nowadays, there has been renewed interest since deterministic-μ is now widespread in industry and it is well understood that any advance in V&V bridging the gap with Monte Carlo approaches will have to come from exploring

probabilistic-μ. Thus, so-called randomized methods [22, 5] and a probabilistic-μ toolbox [3], which evolves from the probabilistic-μ branch and bounds algorithms from [23, 12, 24], have appeared opening the way for further consolidation.

The objective of this paper is to contribute towards the evolution and consolidation of probabilistic-μ by assessing the potential of the toolbox from [3] as well as the quality of the answers through an application to a simple (but relevant) launcher case. The article layout is as follows. First, a brief description of the theory for deterministic and probabilistic μ is given to provide context for their comparison. Then, the launcher thrust vector control (TVC) benchmark is described followed by a section on the results. In order to improve understanding of the results, and due to the criticality of using adequate LFT models, this section presents two different LFT models for the launcher, both considering real uncertainties as well as 1st order bending mode uncertainty, time delay uncertainty and full-complex TVC actuator uncertainty. Then the two models are analyzed in detailed for robust stability with deterministic-μ and a comparison between robust stability, robust performance and worst-case gain provided. The latter connects well with the subsequent section presenting the probabilistic-μ results, which can be perhaps better term probabilistic gain analysis, and which leads to the conclusion.

2 Theory: Deterministic-μ vs Probabilistic-μ

A concept widely used in robust control is the structured singular value μ, which analytically evaluates the robustness of uncertain systems [6, 8, 1]. A key aspect on the application of μ is the development of a proper LFT model. By proper it is meant a model that captures the critical parametric behavior of the nonlinear system under consideration within a complexity that still enables the application of the μ analysis algorithms. In this section, a cursory look at the theory behind LFT modeling, determinstc μ and probabilistic μ are reviewed.

2.1 Linear Fractional Transformations

A LFT is a representation of a system using a feedback interconnection and two matrix operators, $M = [M_{11}\ M_{11};\ M_{11}\ M_{11}]$ and Δ. The matrix M represents the nominal (known) part of the system while Δ contains the unknown, time-varying or uncertain parameters ρ_i. Depending on the feedback interconnection used, there are two possible types of LFTs: lower $F_L(M,\Delta)$ and upper $F_U(M,\Delta)$ (see Fig. 2).

The matrix Δ is unrestricted in form (structured or un-structured) or type (nonlinear, time-varying or constant). It is important to note that unstructured uncertainty at component level becomes structured at system level. The selection of the variable set $\rho(t) \in \Delta$ that captures the behaviour of the nonlinear system is a task that is not always obvious a priori. Indeed, this step is key to obtain a reliable LFT that will

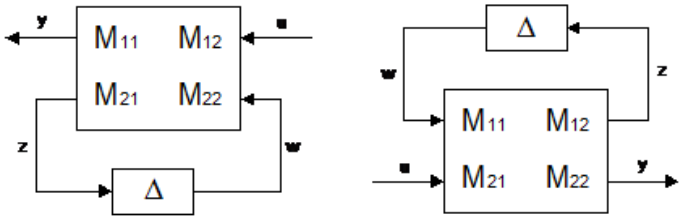

Fig. 2: Lower and upper LFTs

yield relevant and meaningful results and, despite its apparent simplicity, is where most of the LFT modelling effort and ingenuity is focused.

There are several approaches that can be used to obtain a reliable LFT model (see [13, 11, 14, 16, 17] and references therein). The specific approach used in this article is based on the developments from the last two references, which formalized a modeling methodology to transform a general linear parameter varying model into an LFT representation through the use of symbolic manipulations.

2.2 Deterministic-μ

The structured singular value $\mu_\Delta(M)$ of a matrix $M \in C^{n\times n}$ with respect to the uncertain matrix Δ is defined in (1), where $\mu_\Delta(M) = 0$ if there is no Δ satisfying the determinant condition.

$$\mu_\Delta(M) = \frac{1}{\min_\Delta(\sigma(\Delta) : \det(I - \Delta M) = 0)} \tag{1}$$

Note that this definition is given in terms of an $\{M, \Delta\}$ model which is an LFT model where Δ is typically norm-bounded $\|\Delta\|_\infty \leq 1$ (without loss of generality by scaling of M) for ease of calculation/interpretation. In this manner, if $\mu_\Delta(M) \leq 1$ then the result guarantees that the analyzed system, represented by the LFT, is robust to the considered uncertainty level. The structured singular value is a robust stability (RS) analysis but can be used also for robust performance (RP), as this problem can be transformed very straightforward into an RS problem (see [4]).

Since $\mu_\Delta(M)$ is difficult to calculate exactly, the algorithms implement upper and lower bound calculations [1]. The upper bound μ_{upper} provides the maximum size perturbation $|\Delta|_\infty = 1/\mu_{upper}$ for which RS/RP is guaranteed, while the lower bound μ_{lower} guarantees the minimum size perturbation $|\Delta|_\infty = 1/\mu_{lower}$ for which RS/RP is guaranteed to be violated. Thus, if the bounds are close in magnitude then the conservativeness in the calculation of μ is small, otherwise nothing can be said on the guaranteed robustness of the system for perturbations within $[1/\mu_{upper}, 1/\mu_{lower}]$.

In the case the uncertainty set is composed of purely real parameters, $\boldsymbol{\Delta} := \{diag(\delta_1, \delta_2 ... \delta_n) : \delta_i \in \mathbb{R}\}$ then an alternative to equation 1 is as follows:

$$\mu_{\Delta}(M) = \sup_{\Delta \in \boldsymbol{\Delta}, \bar{\sigma}(\Delta) < 1} \rho_r(\Delta M) = \sup_{\Delta \in \boldsymbol{\Delta}, \bar{\sigma}(\Delta) < 1} \bar{\lambda}_r(\Delta M) \tag{2}$$

2.3 Probabilistic-μ

References [21, 19] were the first to use a Monte Carlo probabilistic framework to the robust stability and performance analysis of a system using metrics from classical (i.e. linear) control concepts such as gain/phase margins, s-plane sectors for damping and natural frequency, and time-response metrics for 1st and 2nd order systems. Their approach, called Stochastic robustness analysis (SRA), used the MC probabilistic framework of binomial probability densities and cumulative distributions to obtain a confidence level on the upper and lower bounds (defined based on a specific level of accuracy) on the estimated probability of satisfying an objective.

Subsequently, based on the deterministic-μ developments from [7, 20, 8] and following a similar rationale as the aforementioned two papers, references [23, 12, 24] developed the basic ideas for probabilistic-μ reconciling a probabilistic framework with the linear metric of μ. In reality, probabilistic-μ does not attempt to compute μ using probabilistic methods (which is the objective of randomized algorithms, see [5, 22]) but rather they try to compute hard bounds on the probabilistic gain based on the entire cumulative probability distribution as a function of the entire individual model uncertainty distributions. Notice that this is different, albeit complementary, to the randomized algorithms which following the SRA method use random sampling to estimate the robust probability of satisfying the objective. Reference [3] describes this very accurately and is the basis of the probabilistic-μ theoretical presentation given here.

Probabilistic-μ started with the preliminary investigation of reference [23] which focused on real parameter uncertainty and thus could use the upper bound of equation 2 as the definition of μ:

$$\mu_{\Delta}(M) = \bar{\lambda}_r(\Delta M) \tag{3}$$

Assuming that the probability distribution of Δ for the LFT model $\{\Delta M\}$ is given, then the resulting complementary cumulative distribution of the performance function given below in equation 4 can be obtained using Branch and Bounds (B&B) algorithms. This results in an upper bound to the tail of the distribution for the μ definition of equation 3.

$$P(M, \gamma) = Pr\{\bar{\lambda}_r(\Delta M) \leq \gamma\} \tag{4}$$

A generalization of this result was carried out shortly afterwards in reference [12] considering real and full complex uncertainties, as well as a slightly different

definition for μ. In this reference the idea was to look at μ as the measure of the distance to instability given by the singularity of $det(I-\Delta M)$, which follows more closely the definition of μ as given in equation 1. The resulting probabilistic-μ was then defined as the value of the gain γ for which the probability with confidence level k that Δ is contained in the set $det(\gamma I-\Delta M)\neq 0$ is given by $1-k$:

$$\mu_P(\Delta M,k)=\gamma \quad \text{for which} \quad Pr\{\Delta\in\mathbb{S}_{M,\gamma}\}=1-k \tag{5}$$

where the set $\mathbb{S}_{M,\gamma}$ is the connected region in Δ that contains the origin and for which $det(\gamma I-\Delta M)$ is invertible.

Much more recently, reference [3] has shown the application of a recently developed probabilistic-μ toolbox to the analysis of an UAV flight control. The approach followed uses iterative algorithms to calculate upper and lower hard bounds on the cumulative distribution function (CDF) of the worst-case gain for a system with real, parametric uncertainty but considering the variation over unmodeled dynamics. It is possible to reconcile the main rationale of the approach from this reference with that followed in [21] and [10] in terms of the parallelisms between the binomial CDFs and upper/lower confidence bounds on the probability with the use of the hard upper/lower bounds on μ, which shows the close connection probabilistic-μ offers between Monte Carlo methods and deterministic-μ. In terms of the μ definition used in [3] with respect to those used in [23, 12], the interest is now shifted to obtain hard bounds on the CDF of the function $h(X)$ defined as:

$$h(X)=\max_{\omega\in\mathbb{R}}\ \max_{y\in\mathbb{Y}}\ \bar{\sigma}[F_u(M(j\omega),\Delta(X,y))] \tag{6}$$

where $F_u(M,\Delta)$ represents an upper LFT, see Fig. 2, of the system M with the uncertainty set Δ composed of real parameters X with density probability function p_X and unmodeled dynamics given by the set $\mathbb{Y}$ of stable, norm-bounded, block-diagonal, linear systems. Note that in comparison to the previous μ_p definitions this one is the closest to the original definition in equation 1.

3 Launcher Thrust Vector Control

A launcher thrust vector control (TVC) example is proposed to serve as a simple, yet relevant, study case. The advantage of this case is that it contains some of the main characteristics for atmospheric launchers and facilitates interpretation and understanding of the results. The general characteristics of the study case are:

1. *Simplified planar rigid motion*. The rigid model is a two states / outputs [ψ, $\dot{\psi}$] containing only the launcher aerodynamic A_6 and controllability K_1 terms and with a single input Tn (thrust deflection). The rigid model uncertainty affects the duplet (A_6, K_1), and is the main difference between the two LFT models used in this article -detailed in the next section.

2. *Simplified bending effects*. A single 1st bending mode is used based on a 2nd order model with natural frequency ω_{1B} and damping ζ_{1B}, and assuming 20% real uncertainty for the natural frequency.
3. *Simplified thrust vector control*. The TVC is modelled as a 2nd order dynamic model that includes full complex uncertainty of about 6% ($0.5dB$) introduced as a multiplicative uncertainty weight.
4. *Simplified time delay*. The delay is approximated by a 2nd order Pade model with asymmetric real uncertainty ranging between $[0.1-0.16]$ seconds.
5. *PD attitude controller*. The controller is based on the equivalence of the proportional K_P and derivative K_D gains to a 2nd order system with desired bandwidth ω_{des} and damping ζ_{des} characteristics.
6. *Data at maximum $Q\alpha$ time*. The data used was extracted from a nominal simulation of the VEGACONTROL nonlinear high-fidelity simulator (version VV03) with a real, non-sizing wind profile. The time instance used corresponds to that yielding maximum $Q\alpha$.

The corresponding state-space is given by, where TMC_{PVP} and RMC_{INS} are respectively the bending mode's translational (at pivot point) and rotational (at the inertial navigation system) lengths:

$$A_{LV} = \begin{bmatrix} 0 & 1 & 0 & 0 \\ A_6 & 0 & 0 & 0 \\ 0 & 0 & 0 & 1 \\ 0 & 0 & -\omega_{1B}^2 & -2\zeta_{1B}\omega_{1B} \end{bmatrix}; \qquad B_{LV} = \begin{bmatrix} 0 \\ K_1 \\ 0 \\ -Tn\,TMC_{PVP} \end{bmatrix} \tag{7}$$

$$C_{LV} = \begin{bmatrix} 1 & 0 & -RMC_{INS} & 0 \\ 0 & 1 & 0 & -RMC_{INS} \end{bmatrix}; \qquad D_{LV} = \begin{bmatrix} 0 \\ 0 \end{bmatrix} \tag{8}$$

Focusing on the rigid motion, the plant model $G(s)$ can be represented by:

$$G(s) = \frac{K_1}{s^2 - A6} \tag{9}$$

Define the PD controller as $K(s) = K_P + K_D s$, and assuming unity negative-feedback closed-loop, the following closed-loop transfer function is obtained:

$$T(s) = \frac{L(s)}{I + L(s)} = \frac{G(s)K(s)}{I + G(s)K(s)} = \frac{K_1(K_P + K_D s)}{s^2 + K_1 K_D s + (K_1 K_P - A_6)} \tag{10}$$

Equating the above characteristic equation with an ideal 2nd order system with desired bandwidth ω_{des} and damping ζ_{des}, the following general gain expressions are obtained:

$$K_P = \frac{\omega_{des}^2 + A_6}{K_1}; \qquad K_D = \frac{2\zeta_{des}\omega_{des}}{K_1} \tag{11}$$

Equation 11 shows that given a specific instance of time (from which to obtain $A6$ and $K1$ values), the control designer must only calculate the frequency and damping of the system to obtain the desired behaviour.

4 Results

4.1 Launcher TVC LFT models

In order to provide an assessment on the impact the LFT model may have on the results, two different models are derived based on how the rigid terms A_6 and K_1 are treated. First note that these terms are mathematical variables formed by different physical parameters such as center of gravity x_{CG}, moment of inertia J_{yy} and dynamic pressure $\bar{q}$, in addition to other parameters such as launcher's reference area S_{ref}, yawing coefficient CN_α, center of pressure x_{CP} and pivot reference x_{PVPref}:

$$A_6 = S_{ref}\ \bar{q}\ CN_\alpha \frac{(x_{CP} - x_{CG})}{J_{yy}} \tag{12}$$

$$K_1 = -Tn\ \frac{(x_{CG} - x_{PVPref})}{J_{yy}} \tag{13}$$

The first model, LFT_A uses uncorrelated, non-physical uncertainty parameters (i.e. direct uncertainty on A_6 and K_1) introduced in a multiplicative fashion (e.g $A_6 = A_{6_0}(1 + \sigma_{A_6}\Delta_{A_6})$) where the uncertainty values $\sigma_\bullet$ are chosen based on prior knowledge and rules of thumb (e.g. an over-bounding percentage) and $||\Delta_\bullet|| \leq 1$. Thus, this model represents the standard LFT modelling approach of capturing the state-space matrix coefficients variability across flight conditions and/or physical uncertainty.

For the second model, LFT_B, its characteristics (i.e. uncertainty's model type, level and flags) are chosen based on a methodological analysis of the influence all the uncertain flags implemented in the nonlinear simulator of VEGA have on the physical parameters. This LFT modelling approach is a type of simulation-based first-order Taylor approximation sensitivity analysis whereby the changes of an output of the system (or physical parameter) are assessed in terms of individual changes to each uncertain flag to a first-order (i.e. dropping off uncertainty flags with small influence and only approximating to a first order those with significance influence).

The LFT_B model is composed by *constituent* parameters (i.e. burning time Δ_{dTc} and density Δ_ρ both normalized to 1) correlating the physical terms (J_{yy}, x_{CG}, $\bar{q}$) in an additive fashion, e.g. $J_{yy} = J_{yy0} + \sigma_{J_{yy}dTC}\Delta_{dTc}$ and $x_{CG} = x_{CG0} + \sigma_{x_{CG}dTC}\Delta_{dTc}$. Notice that by *constituent* it is meant those variables that are also directly responsible for the uncertainty in other parameters, e.g. uncertainty in the moment of inertia and center of gravity due to fuel consumption.

In addition, both LFT models include the same bending uncertainty ($\Delta_{\omega_{1B}}$), TVC uncertainty (Δ_{TVC}) and Pade time delay uncertainty ($\Delta_{\tau_{delay}}$). The resulting uncertain parameters repetitions and total LFT order for both models is given in Table 1. Of course the second model is more complex (as measured by the total order) due to the propagation of the constituent uncertainty throughout the system:

Table 1: LFT models

LFT model	$\Delta_{\omega_{1B}}$ $\in[20.08,30.12]$	Δ_{TVC} –	$\Delta_{\tau_{delay}}$ $\in[0.10,0.16]$	Δ_{A6} $\in[-1,+1]$	Δ_{K1} $\in[-1,+1]$	Δ_{dTc} $\in[-1,+1]$	Δ_{ρ} $\in[-1,+1]$	total LFT order
LFT_A	3	1	4	1	1	–	–	10
LFT_B	3	1	4	–	–	5	1	14

A basic grid-based assessment of the sign of the eigenvalues of the closed-loops formed by these LFT models with the same PD controller (described before) is performed next, see Figure 3 . Only the rigid body uncertainty is used, i.e. the uncertainties for the 1st bending model, time delay and TVC are set to a fix (for each LFT model) worst-case value obtained from a robust stability deterministic μ analysis (see next subsection).

For each LFT model a different uncertainty range is used in this eigenvalue analysis each much larger than the $[-1,+1]$ normalized range of the rigid-body parameters. This is done in order to identify the unstable regions as otherwise both LFT closed-loops are robustly stable to changes in the defined rigid-body uncertainty levels -indeed, if the nominal values for ($\Delta_{\omega_{1B}}$, Δ_{TVC}, $\Delta_{\tau_{delay}}$) are used then there are no instabilities.

Figure 3 shows the grid points used and the resulting regions of stability (blue) or instability (red) they determine. The axes for the two plots are scaled equally to facilitate visual comparison of the different regions each grid-based analysis spans. Of course, if all regions were to be connected they will overlap or complement each other, mapping the example's full stability region (i.e. each analysis can be construed as focusing on a specific parameter space region determined by the LFT modeling formulation used).

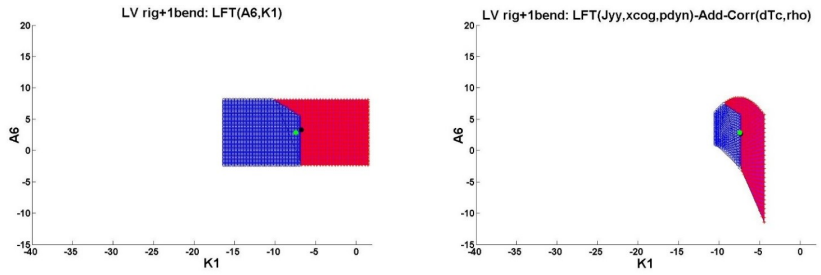

Fig. 3: LFT_A (left) and LFT_B (left) models eigenvalue analysis: stability (blue) and instability (red)

Finally, Figure 4 shows the frequency comparison of the maximum singular values between the two LFT models based on random sampling of the uncertainty set

(yellow lines), the nominal value (solid black line with '*' markers) and the worst-case gain (solid red line with '+' markers). It is clear that the general behaviour for both LFT models is similar but that each have specificities arising from the different type of uncertain model, parameters and ranges used.

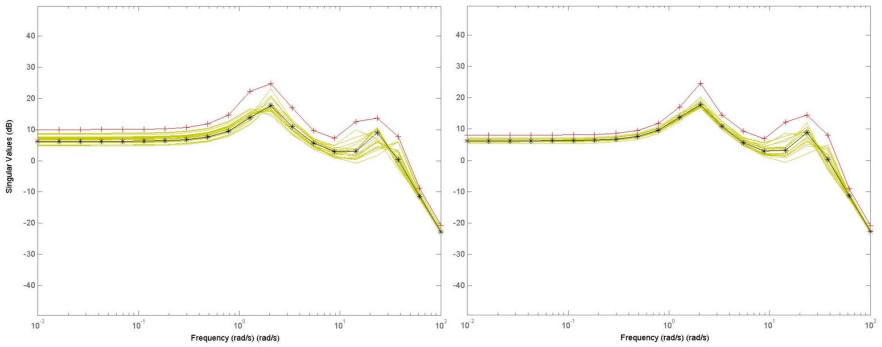

Fig. 4: LFT_A (left) and LFT_B (left) maximum singular value analysis: random (yellow), nominal (black *) and worst-case gain (red +)

4.2 Deterministic μ

4.2.1 Robust stability comparison

Using the command *robuststab* from the Robust Control toolbox in Matlab [1] it is straightforward now to perform a robust stability (RS) analysis for each LFT model described before. Of course, finding the exact value of μ has been shown to be NP-hard except for a few special cases. Thus, all μ algorithms work by searching for upper and lower bounds, which in practice and after several decades of experience with diverse systems are known to be typically close. Recall that the lower bound μ_{LB} provides a worst-case combination of uncertain parameters of minimum size $||\Delta_{LB}|| = 1/\mu_{LB}$ guaranteed to make the analyzed closed-loop unstable, while the upper bound μ_{UB} provides a guarantee for the maximum size of the uncertainty for which the closed-loop is stable. If the gap between the bounds is non-negligible then nothing can be said on whether there are other combinations of size $||\Delta||$ smaller than $||\Delta_{LB}||$ that make the system unstable or larger than $||\Delta_{UB}|| = 1/\mu_{UB}$ that make it stable.

In addition, it is well-known that μ-analysis with all the uncertain parameters real may present discontinuities when calculating the lower bound. This is typically avoided by performing a mixed real/complex μ-analysis requiring only that at least one of the uncertain parameters used in the LFT model is complex. In the present case due to the full complex uncertainty used for the TVC model there is no need to "complexify" the uncertainty set.

Figure 5 shows the RS upper and lower bounds for each LFT model using the full uncertainty set. It is interesting to note that the μ bounds are very similar, although between each model there is a slight difference, see the bump in the frequency region $[1-3]$ radians/seconds and the smaller value for the lower bounds of LFT_B in the lower frequency region. Recall that one of the main differences in the construction of the LFT models is the use of a multiplicative type of uncertainty model for LFT_A and of an additive model for LFT_B . Still, it is noticeable that for this study case the two LFT models allow to obtain very tight results for the bounds, especially for the peaks in the low frequency (associated to the launcher LF margin) and in the higher frequency (associated to the 1st bending mode).

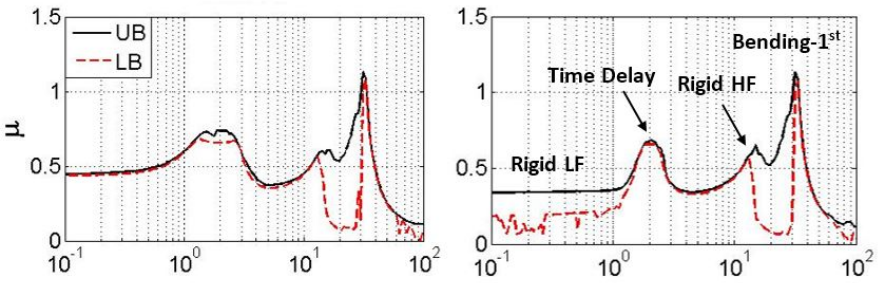

Fig. 5: RS-μ bounds for full uncertainty set: LFT_A (left) and LFT_B (right)

Since both the upper and lower bounds are very tight and above $\mu = 1$, this means that the μ-RS analysis has been able to detect a worst-case combination within the defined uncertainty level that will drive the system unstable. It is easy to see that this worst-case arises from the introduction of uncertainty in the bending mode -clearly seen since the μ violation is around the frequency of the 1st bending mode.

Although typically only the worst-on-worst (i.e. the highest peak) uncertainty combination is used, it is remarked that a de-stabilizing perturbation of size $||\Delta|| < 1$ can be obtained for each frequency tested that yields $\mu_{LB} \geq 1$. Thus, a direct region-based identification of worst-cases may be performed although this requires careful assessment of the worst-cases.

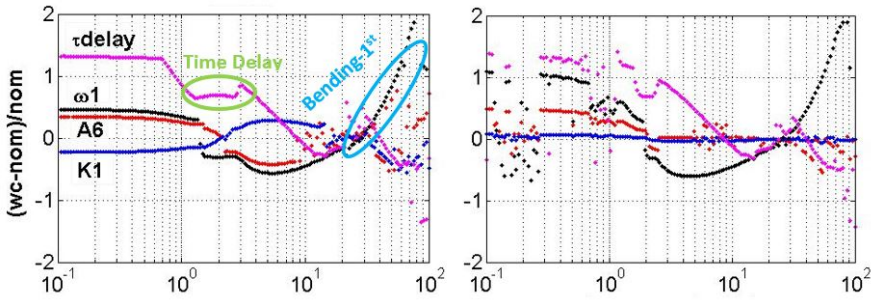

Fig. 6: RS-μ worst-case full uncertainty set across frequency: LFT_A (left) and LFT_B (right)

Table 2 shows the values of (A_6, K_1) resulting for the two runs of RS-μ worst-case for each model. The μ-analysis algorithm underlying the *robuststab* command, i.e. mussv, uses a random initialization scheme so each run may yield a different results. Notice that the (A_6, K_1) values are similar, as well as those for the ($\Delta_{\omega_{1B}}$ and $\Delta_{\tau_{delay}}$), across model and run but that there is a slight difference on the LFT_B uncertainty combinations for each run and a much greater difference for the LFT_A uncertainties.

Table 2: Robust Stability worst-case combinations

LFT model	A_6	K_1	$\Delta_{\omega_{1B}}$ $\in[20.08,30.12]$	Δ_{TVC} –	$\Delta_{\tau_{delay}}$ $\in[0.10,0.16]$	Δ_{A6} $\in[-1,+1]$	Δ_{K1} $\in[-1,+1]$	Δ_{dTc} $\in[-1,+1]$	Δ_{ρ} $\in[-1,+1]$
LFT_A	2.5320	-7.2471	29.7989	full	0.1558	-0.8123	-0.2287	–	–
	3.2763	-6.7300	29.7874	full	0.1557	0.9085	-0.9260	–	–
LFT_B	2.6109	-7.3238	29.8005	full	0.1559	–	–	-0.9286	-0.9104
	2.6100	-7.3238	29.8005	full	0.1559	–	–	-0.9286	-0.9147

4.2.2 Worst-case gain, robust stability and robust performance comparison

As aforementioned in subsection 2.2, μ allows also to analyze the robust performance (RP) of a system by posing this problem as a robust stability (RS) problem through the use of an additional fictitious uncertainty. The analysis is directly performed using the command *robustperf* from the toolbox [1], which calculates the RP margin of an uncertain system.

In addition, another type of robust analysis is available from the toolbox [2] called worst-case gain (WCG) – performed with the command *wcgain* in the same fashion as the previous two. It calculates upper and lower bounds on the worst-case peak gain of the uncertain system –note that for MIMO systems this refer to the maximum singular value peak gain of the frequency response matrix over the uncertainty set. For comparison to the bounds from the deterministic μ, the option that calculates the worst-case peak across frequency and over the uncertainty set is used.

For the present study case, the calculation of the worst-case gain takes much more time than the *robuststab* or the *robustperf* algorithms. This seemed to be associated to the number of parameters and total repetitions of the LFT model as well as to the number of frequency points used for the analysis. Indeed, for both LFT models using the full uncertainty set and 200 frequency points (equally distributed in the log-space), the time it took to obtain the worst-case gain bounds was almost 100 times more (i.e. 33 minutes as opposed to the 14 seconds for the μ analyses). These two causes, LFT complexity and frequency grid refinement, will also have a more prohibitively magnifying effect for the probabilistic μ. Not only that, the quality of the worst-case gain became discontinuous and in the aforementioned instance, i.e. 200 frequency points for the full uncertainty set, the value of the gain for the LFT_A model was about 900 and that for the LFT_B model was infinite. This experience is in contrast to the expectation of using *wcgain* which is supposed to not suffer from

discontinuities effect as for example the *robuststab* analysis, it is an issue for future research.

In order to provide a comparison, the results from the three robust analyses discussed above are shown in Figure 7 for both LFT models and the full uncertainty set. The RS and RP algorithms used 200 frequency points while the WCG used 20 due to the limitation just mentioned. Notice that as expected the RS upper bounds are smaller than the RP bounds, and these are smaller than those for WCG. Also, both models produce similar results. It is interesting to note that now the highest peaks for the RP and WCG bounds are around the launcher HF-margin frequency region and not around that for the 1st bending. Table 3 gives the worst combinations for the RS, RP and WCG analyses corresponding to the previous figure.

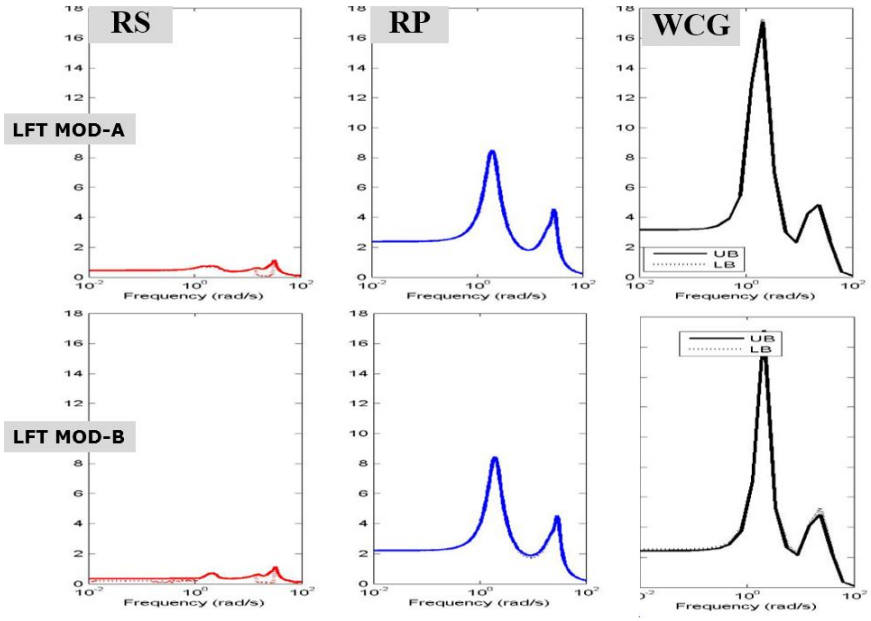

Fig. 7: WCG/RS-μ/RP-μ bounds for full uncertainty set: LFT_A (top) and LFT_B (bottom)

Table 3: Robust performance (RP) and worst-case (WCG) combinations

LFT model	$\Delta_{\omega_{1B}}$ $\in[20.08,30.12]$	Δ_{TVC} –	$\Delta_{\tau_{delay}}$ $\in[0.10,0.16]$	Δ_{A6} $\in[-1,+1]$	Δ_{K1} $\in[-1,+1]$	Δ_{dTc} $\in[-1,+1]$	Δ_{ρ} $\in[-1,+1]$
LFT_A RP	29.7874	full	0.1557	0.9260	-0.9260	–	–
RS	25.7336	full	0.1233	0.1195	-0.1195	–	–
WCG	21.3313	full	0.1600	-0.5462	-0.1231	–	–
LFT_B RS	29.8005	full	0.1559	–	–	-0.9286	-0.7959
RP	25.6897	full	0.1233	–	–	0.1195	-0.1176
WCG	20.1062	full	0.1600	–	–	1.0000	-0.6509

It is clear that both LFT models are adequate for robust deterministic μ analysis, although when the full uncertainty set is used the calculation of the worst-case gain as currently implemented suffers from exponential time issues. The main apparent difference between the models resides in the LFT_B model being of slightly higher dimension (e.g. for the full uncertainty set both having 5 uncertain parameter but LFT_B a total of 14 repetitions compared to 10 for the LFT_A model, while when no bending uncertainty is used the dimension is 11 versus 7 –and both models dropping to 4 uncertain parameters in this case).

4.3 Probabilistic μ

In this section, the probabilistic μ algorithm, μ_{prob}, as described in reference [3][1] is applied to the launcher case. Equivalent to the previous robust analyses, the implementation uses a single command *probgain* and necessitates of an uncertain LFT model and a frequency grid, plus in addition probabilistic-μ algorithmic specifications such as: the CDF bound thresholds, the definition of the parameter uncertainty PDFs, the maximum number of branches allowed for the search, and the maximum time allowed for the calculation. The output provides lower and upper bounds on the CDF of the probability of achieving a level of performance gain. The upper bound is in turn always bounded from above by the worst-case gain obtain from *wcgain*, and should coincide when the CDF probability is 1. In addition, as expected from Figure 7, the μ_{RS} / μ_{RP} upper and lower bounds values, which can be equated to the robustness or performance guaranteed gains, will always be also bounded from above by the worst-case gain.

Figure 8 shows the probabilistic-μ CDF bounds (blue-solid for the lower and blue-dashed for the upper) for the two LFT models, LFT_A in the top row and LFT_B in the bottom, and under two uncertainty sets, full Δ on the left column and the same set without the bending uncertainty on the right column. The worst-case gain obtained for each LFT model/uncertainty-set using the previous *wcgain* command is also plotted as a vertical solid line on the right of the figure (always upper bounding the CDF upper bound). In addition, in order to compare the validity and conservativeness of the CDF bounds with respect to Monte Carlo, ten sampling campaigns are performed for each LFT model/uncertainty-set using 100 random samples. These are plotted in cyan-solid and they should be located mostly within the CFD bounds which represents an indication of the validity of the probabilistic-μ results. Notice that if they cover most of the gap between the CFD bounds this will indicate a non-conservative result of the latter. This non-conservativeness can be interpreted as an indication that the worst-cases identified with deterministic μ for a given gain-level will have a high probability of occurring. On the other hand, if the MC results do not widespread across the CFD bounds it can also be interpreted as an indication of the limited value of MC to detect worst-cases or maximum/minimum combinations.

[1] The associated toolbox was developed and kindly provided by Dr. G.J. Balas and co-workers [3].

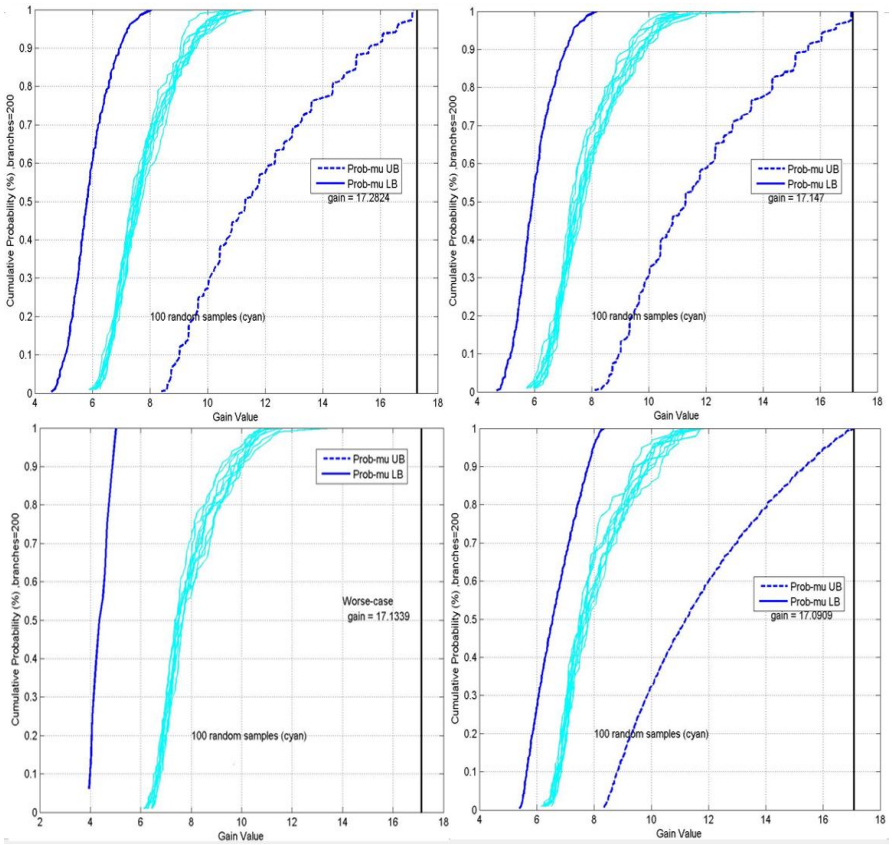

Fig. 8: Prob-μ bounds (blue) and MC (cyan) CDFs plus WCgain (vertical black): 20 freq-pts, LFT_A (top-row) vs LFT_B (bottom row) and Full Δ (left column) vs No Bending Δ (right column)

Before examining Figure 8 in more detail, note that the presented μ_{prob} results use 20 frequency points since as mentioned in the previous section for the case of 200 frequency points and full Δ, the worst-case gain yielded values of 900 and infinite respectively for the LFT_A and LFT_B models. Not only this, but they took a relatively long time to complete in comparison to the deterministic μ analyses (see subsequent Tables 4 and 5), which translated in even longer time for μ_{prob} –and in the case of the LFT_B model with full Δ the calculation had to be stopped after 5 hours. In the Figure this difficulty is still seen, since for that case (bottom-left plot) the probabilistic CFD μ upper bound was not found. The plots in the Figure show that the difference between LFT models, and actually between uncertainty sets, does not have an impact on the worst-case gain value or the CDF profile and value –except for the upper bound of the case just mentioned. For these four cases, the MC campaign yields a very compact band typically located close to the lower

CDF bound. This means that potentially either the MC is conservative or the μ worst-cases are unlikely for gains below 4 and above 10 (but up to 18). A different type of interpretation is possible by for example, looking at the 90% probability level of the top-left plot (i.e. LFT_A model with full Δ). It crosses the Monte Carlo sampled band around a gain value of 9.7, this means that for the current sampling (consisting of 100 random samples) there are 10% of uncertain cases that have a gain larger than 9.7, but looking at the probabilist μ FCD bounds the interpretation is that there are 10% of the uncertain cases with a guaranteed gain value higher than 7 and lower than 15.6.

Next, the uncertainty set used was reduced to the two real parametric parameters: (A_6, K_1) for LFT_A and (Δ_{dTc}, Δ_ρ) for LFT_B. This resulted in a total LFT dimension of 2 for LFT_A and 6 for LFT_B. Thus, this will allow evaluating the μ_{prob} algorithm in terms of speed improvements as well as to assess if the CDF calculations map the expected lower worst-case gain (for this uncertainty sets the *wcgain* yielded values around 8). In addition, in order to assess also the effect of "complexification" (a useful computational trick to deal with pure real problems in μ analysis [1]) one of the uncertain parameters is made complex by 1%.

Figure 4 shows the results of this evaluation for the LFT_A model, on the left for the pure real uncertainty and on the right for the mixed real-complex. Notice that the "complexification" has resulted in less than 0.1% difference for the worst-case gain (and relatively same variation for the CFD). In this case, due to the lesser complexity of the LFT models the bounds show almost non-conservative results with respect to the MC campaigns indicating that the worst-cases likelihood will be high. Similar results were obtained for model LFT_B except that the worst-case gain threshold shifted to the left by about 3%, which means that the difference in generating the LFT model has much greater impact than the "complexification" (as expected).

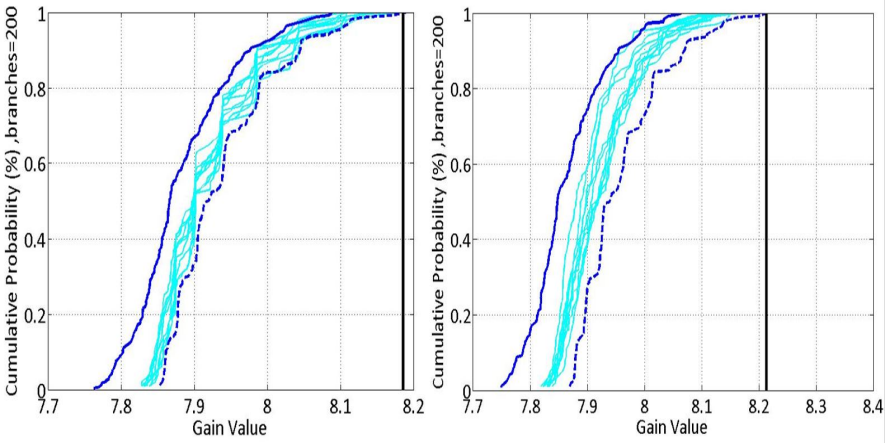

Fig. 9: Prob-μ bounds (blue) and MC (cyan) CDFs plus WCgain (vertical black) for LFT_A model: 200 freq-pts but only $\Delta = (A_6, K_1)$ - -pure real (left) and mixed real-complex (right)

The times required to compute the deterministic μ RS and RP bounds, the worst-case gain and the probabilistic μ CFDs are given in Tables 4 and 5. Both tables show the times to perform the calculations for: (i) 200 versus 20 frequency points, and (ii) the LFT_A versus LFT_B models. The difference between the tables is on the uncertainty sets used with Table 4 showing the computational time for the full Δ and Table 5 for the no-bending uncertainty set (i.e. the LFT models/uncertainty-sets from Figure 8).

Note that the μ RS and RP calculations are very quick and consistent in time regardless of the LFT model, uncertainty set or number of frequency points. When the preliminary deterministic μ algorithm implementations first appeared these three issues limited severely its applicability and resulted in very long computational times, but as it is clear nowadays the algorithms and implementations greatly improved and are now in the matter of seconds (although might still be daunting for some systems with pure real uncertainty, many parameters, e.g. > 20, and high total LFT dimension, e.g. > 50). The worst-case gain calculation shows to be highly depending for this launcher case on the frequency grid used (1868.70 seconds versus 137.70 for LFT_B) but also the actual LFT model (102.81 seconds versus 1868.70 for 200 freq-points) and uncertainty set (102.81 versus 43.35 seconds for LFT_A and 200 freq-points). For the case of μ_{Prob}, and since it is based on *wcgain*, the situation is as that of deterministic μ at the beginning with some cases taking prohibitively long times (i.e. LFT_B with full Δ) and on average taking too long for standard use in the control design cycle –although possibly still acceptable for limited model complexity during analysis in conjunction with Monte Carlo campaigns.

Table 4: Deterministic and Probabilistic μ computational comparison (seconds): Full Δ
$LFT_A = \{5$ parameters, 10 repetitions$\}$ and $LFT_B = \{5$ parameters, 14 repetitions$\}$

	LFT model	RS-μ	RP-μ	WCgain	Prob-μ
200	LFT_A	12.47	13.72	102.81	6191.16
freq-pts	LFT_B	13.85	14.36	1868.70	stopped after 5hrs
20	LFT_A	9.12	10.03	9.12	688.58
freq-pts	LFT_B	9.65	10.22	137.70	6642.01

Table 5: Deterministic and Probabilistic μ computational comparison (seconds): no bending Δ
$LFT_A = \{4$ parameters, 7 repetitions$\}$ and $LFT_B = \{4$ parameters, 11 repetitions$\}$

	LFT model	RS-μ	RP-μ	WCgain	Prob-μ
200	LFT_A	13.83	10.74	43.37	3828.21
freq-pts	LFT_B	13.06	12.04	141.45	6266.44
20	LFT_A	9.96	8.36	3.44	283.06
freq-pts	LFT_B	9.44	7.77	10.63	521.77

5 Conclusions

In this article a comparison of the standard μ algorithm [1, 2] and its probabilistic counterpart [23, 12, 24], as implemented by Prof. Balas and co-workers [3], is performed using as a study case a simple, yet relevant, launcher thrust vector control example. The results show the potential to bridge the results from deterministic μ with those from Monte Carlo campaigns providing a potentially high impact axis of improvement on current worst-case approaches towards their accepted use in V&V and certification processes.

In terms of the algorithmic implementation of μ_{prob}, the situation is similar to when first appeared the preliminary implementations of deterministic μ. That is, in some cases it takes prohibitively long and on average takes too long for standard use in the control design cycle –although possibly still acceptable for limited model complexity during analysis in conjunction with Monte Carlo campaigns. In conclusion, additional investigations into more efficient and fast algorithmic implementations of μ_{prob} and the development of a consolidated toolbox (through improved coding and widespread use) has the potential to bridge the aforementioned gap and could in time become as widespread in the academic world and industry as deterministic μ is nowadays.

Acknowledgements This work was funded by ESA-ESTEC Contract No. 4000111052/14/NL/GLC/al within the project "Analytic Stochastic Time Varying Mu Analysis for the VEGA GNC".

References

1. Balas, G.J., Doyle, J.C., Glover, K., Packard, A., Smith, R., "μ-Analysis and Synthesis Toolbox," Musyn-Mathworks, 1998
2. Balas, G.J., "Robust Control Toolbox"
3. Balas, G.J., Seiler, P.J., Packard, A.K., "Analysis of an UAV Flight Control System using Probabilistic μ," AIAA Guidance, Navigation and Control Conference, Portland, USA, 2012
4. Bateman, A., Ward, D., Balas, G., "Robust/Worst-Case Analysis and Simulation Tools," AIAA Guidance, Navigation and Control Conference, San Francisco, USA, 2005
5. Calafiore, G., Dabbene F., Tempo, R., "Research on Probabilistic Methods for Control System Design," Automatica, Vol. 47, 2011
6. Zhou, K., Doyle, J.C., and Glover, K. Robust and Optimal Control. Prenticel-Hall, Englewood Cliffs, NJ, 1996.
7. Doyle, J., Analysis of feedback systems with structured uncertainties, IEE Proceedings, vol. 129-D, pp. 242-250, 1982
8. Doyle, J., Packard, A., Zhou, K., Review of LFTs, LMIs, and , IEEE Conference on Decision and Control, 1991
9. Ganet, M., Bourdon, J., Gelly, G., Nonlinear and robust stability analysis for ATV rendezvous control, AIAA Guidance, Navigation and Control Conference, USA, 2009
10. Hanson, J.M, Beard, B.B., "Applying Monte Carlo Simulation to Launch Vehicle Design and Requirements Verification," AIAA Guidance, Navigation and Control Conference, Toronto, Canada, 2010
11. Hansson, J., Using Linear Fractional Transformations for Clearance of Flight Control Laws, MS Thesis Linkpings University (Sweden), LiTH-ISY-EX-3420-2003, October 2003.

12. Khatri, S., Parrilo, P.A., "Guaranteed Bounds for Probabilistic μ," IEEE Conference on Decision and Control, Tampa, USA, 1998
13. Lambrechts, P., Terlouw, J., Bennani, S., Steinbuch, M., Parametric Uncertainty Modeling using LFTs, American Control Conference, San Francisco, USA, 1993
14. Magni, J.F., "Linear Fractional Representation Toolbox: Modeling, order Reduction, Gain Scheduling," TR 6/08162 DCSD, ONERA, Toulouse, France, January, 2004
15. Marcos, A., Balas, G.J., Development of Linear Parameter Varying Models for Aircraft, AIAA Journal of Guidance, Control, and Dynamics, vol. 27, no. 2, pp. 218-228, 2004
16. Marcos, A., Bates, D.G., Postlethwaite, I., A Symbolic Matrix Decomposition Algorithm for Reduced Order Linear Fractional Transformation Modelling, Automatica, vol. 43, no. 7, pp. 1125-1306, 2007
17. Marcos, A., Mantini, V., Roux, C., Bennani, S., "Bridging the Gap between Linear and Nonlinear Worst-Case Analysis: An Application Case to the Atmospheric Phase of the VEGA Launcher", IFAC ACA, 2013
18. Menon, P.P., Prempain, E., Postlethwaite, I., Bates, D.G., Nonlinear Worst-Case Analysis of an LPV Controller for Approach-Phase of a Re-Entry Vehicle, AIAA Guidance, Navigation and Control Conference, 2009
19. Ray, L.R., Stengel, R.F., "Stochastic Measures of Performance Robustness in Aircraft Control Systems," AIAA Journal of Guidance, Control and Dynamics, v15, n6, 1992
20. safonov, M., "Stability margins of diagonally perturbed multivariable feedback systems," IEE Proceedings, vol. 129-D, pp. 251-256, 1982
21. Stengel, R.F., Ray, L.R., "Stochastic Robustness of Linear Time Invariant Control Systems," IEEE Transactions on Automatic Control, v36, n1, 1991
22. Tempo, R., Calafiore G., Dabbene, F., "Randomized Algorithms for Analysis and Control of Uncertain Systems," Springer-Verlag, London, 2005
23. Zhu, X., Huang, Y., Doyle, J., "Soft vs. Hard Bounds in Probabilistic Analysis," IEEE Conference on Decision and Control, Kobe, Japan, 1996
24. Zhu, X., "Improved Bounds Computation for Probabilistic μ," American Control Conference 2000